Published in final edited form as:
Acta Biomater. 2010 January ; 6(1): 29–38. doi:10.1016/j.actbio.2009.07.009.

Modular scaffolds assembled around living cells using poly (ethylene glycol) microspheres with macroporation via a non-cytotoxic porogen

Evan A. Scott[1], **Michael D. Nichols**[1], **Rebecca Kuntz-Willits**[2], and **Donald L. Elbert**[1,*]

[1] Department of Biomedical Engineering and Center for Materials Innovation, Washington University in St. Louis, St. Louis, MO, USA

[2] Department of Biomedical Engineering, St. Louis University, St. Louis, MO, USA

Abstract

Modular, bioactive, macroporous scaffolds were formed by crosslinking poly(ethylene glycol) (PEG) microspheres around living cells. Hydrogel microspheres were produced from reactive PEG derivatives in aqueous sodium sulfate solutions without the use of surfactants or copolymers. Microspheres were formed following thermally induced phase separation if the gel point was reached prior to extensive coarsening of the PEG-rich domains. Three types of PEG microspheres with different functionalities were used to form scaffolds. One type of PEG microsphere provided mechanical support, the second type provided controlled delivery of the angiogenesis-promoting molecule, sphingosine 1-phosphate (S1P), and the third type served as a slowly dissolving non-cytotoxic porogen. Scaffolds were formed by centrifuging microspheres in the presence of HepG2 hepatoma cells, resulting in a homogenous distribution of cells. During overnight incubation at 37° C, the microspheres reacted with serum proteins in cell culture medium to stabilize the scaffolds. Within two days in culture, macropores formed due to the dissolution of the porogenic PEG microspheres, without affecting cell viability. Gradients in porosity were produced by varying the buoyancy of the porogenic microspheres. Conjugated RGD cell adhesion peptides and delivery of sphingosine 1-phosphate promoted endothelial cell infiltration through macropores in the scaffolds. The scaffolds presented here differ from previous hydrogel scaffolds in that: 1) cells are not encapsulated in hydrogel, 2) macropores form in the presence of cells, and 3) scaffold properties are controlled by the modular assembly of different microspheres that perform distinct functions.

Keywords

poly(ethylene glycol); hydrogel; modular scaffold; tissue engineering; LCST; cloud point; microsphere; endothelial; sphingosine 1-phosphate; HepG2

*To whom correspondence should be addressed: Donald L. Elbert, Department of Biomedical Engineering, Campus Box 1907, One Brookings Dr. Washington University, St. Louis, MO 63130, Ph: (314) 935-7519, Fax: (314) 935-7448, E-mail: elbert@biomed.wustl.edu.

Introduction

Hydrogels made from synthetic polymers are promising as scaffolds for tissue engineering [1,2]. PEG-based scaffolds exhibit a high resistance to non-specific protein adsorption and are easily modified with peptides and proteins to impart biological functions such as cell adhesion or cell-initiated degradability [3]. However, bulk PEG hydrogels effectively encapsulate cells in polymer [3,4], potentially impacting cell survival, proliferation and migration. Porosity at multiple length scales may thus be desirable, with smaller pores providing a niche for functional cells and larger pores permitting vascularization [5]. Such multi-scale porous hydrogels can be formed with a variety of porogens [6–12], but a need exists for porogens that rapidly dissolve without compromising cell viability. A non-cytotoxic porogen would permit incorporation of cells at the time of scaffold formation, potentially leading to a more homogenous distribution of cells compared to cell seeding after scaffold formation.

Modular assembly of different types of microparticles is also desirable to allow versatility in engineering the properties of the scaffold [13–19]. However, the scalability of many microparticle production techniques (e.g. micromolding, microfluidics, 3D printing) may be a concern due to the large number of microparticles required to form scaffolds of sufficient size for practical applications [16,20–25]. Formation of hydrogel microspheres in solution addresses the issue of scalability but typically requires the use of organic solvents and surfactants in a two-phase system. These additives allow fine control over the size of microspheres but may be difficult to remove later, potentially affecting biocompatibility. Microspheres can be formed in water by copolymerizing PEG with polymers that exhibit a lower critical solution temperature (LCST) near physiological temperature, e.g. poly(N-isopropylacrylamide) [26,27]. However, poly(N-isopropylacrylamide) promotes protein adsorption at physiological temperature [28], and thus maximizing the concentration of PEG in the microspheres is desirable [29,30].

The LCST/cloud point of low molecular weight PEG is above the boiling point of water but is greatly decreased by kosmotropic salts [31–33]. An advantage of using salts for PEG phase separation is their easy removal by buffer exchange after microsphere formation. Phase separation above the cloud point initially leads to the formation of small spherical domains that grow in size over time (i.e. coarsen). Coarsening eventually results in the formation of two distinct phase-separated layers due to differences in the densities of the phases. Hennink and colleagues found that polymerization of vigorously mixed emulsions of phase-separated PEG/magnesium sulfate solutions led to the formation of large aggregates of PEG microspheres, which was ascribed to the low viscosity of the solution [34]. Here, we report that PEG microspheres with diverse functionalities can be formed in aqueous solutions without surfactants by timing the gel point to occur early in the coarsening process in the absence of mixing (Fig. 1a). The microspheres were assembled into scaffolds possessing characteristics that together may advance tissue engineering strategies: modularity, biological activity and porosity at multiple length scales (Fig. 1b). Furthermore, degradable 100% PEG microspheres are non-cytotoxic, permitting macropore formation in the presence of living cells.

Materials and Methods

PEG derivatives

Unless otherwise noted, all reagents were purchased from Sigma-Aldrich. Eight-arm PEG-OH (PEG_8-OH; mol. wt. 10,000; Shearwater Polymers, Huntsville, AL) was used to synthesize PEG_8-vinylsulfone (PEG_8-VS), PEG_8-amine, and PEG_8-acrylate as previously described [35,36]. Stock solutions of PEG_8-VS, PEG_8-amine, PEG_8-acrylate, and fatty acid-free bovine serum albumin (BSA) solutions were prepared at 20%(w/v) in Dulbecco's phosphate buffered saline (Pierce) and sterile filtered with 0.22 μm syringe filters. For fluorescent labeling, stock

solutions of PEG_8-amine or BSA in PBS were reacted with a 10 mg/mL solution of Dylight-488 or Dylight-633 (Pierce) in dimethylformamide at a 100:1 molar ratio of PEG:dye or BSA:dye overnight at room temperature. All solutions are reported as weight/volume percent.

Dynamic light scattering (DLS)/Zeta potential

Dynamic light scattering/photon correlation spectroscopy (DLS/PCS; 90Plus Particle Size Analyzer, Brookhaven Instruments, Holtsville, NY) was performed at a scattering angle of 90° and wavelength of 658 nm. Calculation of the mean effective diameter (d_{PCS}) and statistical analysis of the results were performed using Brookhaven Instruments Particle Sizing Software (version 2.34, Brookhaven Instruments). Zeta potentials of microspheres were measured on the DLS instrument in 10 mM sodium phosphate at the listed pHs.

Microsphere fabrication – general protocol

PEG_8-VS/PEG_8-amine microspheres were fabricated from solutions of PEG_8-VS and PEG_8-amine pre-reacted below the cloud point at 37°C at a concentration of 20%(w/v) PEG in PBS. The solutions were reacted to $d_{PCS} \cong 100$ nm measured by DLS. Pre-reacted solutions could be stored at −80°C for at least five months. Pre-reacted solutions were diluted to 2%(w/v) PEG at room temperature with PBS and PBS + 1.5 M sodium sulfate to achieve a final sodium sulfate concentration of 0.6 M and volume of 50 μL. The solutions were then heated above the cloud point to 37°C for 45 min unless otherwise stated. Suspensions of microspheres were buffer exchanged into PBS 2x to remove the sodium sulfate, diluting the microsphere solution 3:1 with PBS, titurating and centrifuging at 14,100*g* for 2 min. PEG_8-VS /BSA microspheres were formed by pre-reaction of PEG_8-VS and BSA (12%(w/v) BSA + 8%(w/v) PEG in PBS, 37°C, reacted to $d_{PCS} \cong 100$ nm), dilution10x at room temperature to obtain PBS + 0.65 M sodium sulfate and reaction for 25 min at 37°C. The number of reactive amines per BSA was assumed to be 36 [37]. PEG_8-acrylate and PEG_8-amine were pre-reacted (20%(w/v) PEG in PBS, 37°C, reacted to $d_{PCS} \cong 100$ nm), diluted 10x at room temperature to obtain PBS + 0.45 M sodium sulfate and reacted for 3–10 min at 95°C. To visualize the porous structure of the microspheres, larger microspheres were produced as follows. The microspheres were formed as described above, except in PBS + 0.8 M sodium sulfate to cause phase separation at room temperature. Samples were held above the cloud point at room temperature for 5 min prior to reaction at the temperature and time stated above.

Microsphere fabrication for scaffolds

S1P was dissolved in methanol at 0.5 mg/mL and divided into 287 nmol aliquots in Eppendorf tubes. The methanol solutions were dried under nitrogen. The tubes were filled with 20% (w/v) BSA in PBS (1 nmol S1P/mg BSA) and rotated at 37°C until S1P was completely solubilized. Pre-reacted solutions of PEG_8-VS/PEG_8-amine (2:1 VS:amine, $d_{PCS} \cong 50$ nm, 20%(w/v) PEG) or PEG_8-VS/BSA/S1P (2:1 VS:amine, $d_{PCS} \cong 50$ nm, 8.5%(w/v) BSA + 11.5%(w/v) PEG) were reacted for 30 min at 37°C with RGD peptide (sequence: GCGYGRGDSPG, Genscript Corp.) at an RGD concentration of 5.5 mM [37]. Pre-reacted PEG_8-VS-RGD/PEG_8-amine solutions (25 μL) were diluted 10x to obtain PBS + 0.6 M sodium sulfate and heated for 45 min at 37°C. Pre-reacted PEG_8-VS-RGD/BSA/S1P solutions (25 μL) were diluted 10x to obtain PBS + 0.65 mM sodium sulfate. Microspheres were formed by incubation of this solution for 25 min at 37°C. Pre-reacted PEG_8-acrylate/PEG_8-amine solutions (1:1 acrylate:amine, $d_{PCS} \cong 100$ nm, 20%(w/v) PEG, 25 μL) were diluted 10x to obtain PBS + 0.45 mM sodium sulfate. Microspheres with low, medium, or high densities were formed by incubation of this solution at 95°C for 3 min, 5 min, or 10 min, respectively. Microsphere suspensions were buffer exchanged first into PBS and then into endothelial growth medium (EGM; MCDB 131 medium supplemented with 10 ng/mL epidermal growth factor, 10 mg/

mL heparin,1.0 mg/mL hydrocortisone, 1% penicillin–streptomycin, 2% FBS, and 12 mg/mL bovine brain extract; Clonetics).

Scaffold assembly and cell seeding

PEG_8-VS/PEG_8-amine microspheres, PEG_8-VS/BSA microspheres and PEG_8-acrylate/PEG_8-amine microspheres (1:1:1 of washed microsphere solutions in EGM) were combined and briefly mixed by tituration with $5x10^5$ HepG2 cells in EGM in UV/vis cuvettes (Brookhaven Instruments Corporation) to a final volume of 1 mL. Microspheres and cells were centrifuged for 10 min at 1000*g*. Scaffolds were incubated for 48 h at 37°C followed by replacement of the medium with fresh EGM containing $5x10^5$ endothelial cells. Live/dead assays were performed by incubating scaffolds for 30 min at 37°C with EGM containing 12 μM fluorescein diacetate (Sigma) and 250 μM ethidium bromide (Pierce).

Confocal microscopy

Fluorescence microscopy was performed with a Nikon Eclipse C1/80i confocal microscope. Suspensions of fluorescently-labeled microspheres were imaged on glass microscope slides (Corning Inc.) with a 20X objective (0.45 DIC L WD 7.4). Scaffolds were imaged in EGM and within UV/vis cuvettes with a 10X objective (0.3 *DIC L/N1 WD 16.0)*. Images were processed and rendered in 3D using EZ-C1 3.70 FreeViewer software (Nikon Instruments Inc.).

Rheometry

Storage (G') and loss (G") moduli of bulk hydrogels and scaffolds were measured at room temperature by oscillatory shear rheometry (25 mm parallel plate) on a rheometer (RFS3, Rheometric Scientific). Viscoelasticity was measured at 5% strain within a frequency range of 1–100 Hz. Scaffolds (1 mm thickness) were formed from PEG_8-VS/PEG_8-amine microspheres (2:1 VS:amine) as above, with centrifugation in silanized (Sigmacote) glass vials (25 mm diameter). Bulk hydrogels were prepared *in situ* on the surface of the 25 mm parallel plate by mixing 200 mg/mL solutions of PEG_8-VS (200 μL) and PEG_8-amine (200 μL) in PBS, pH 10.0 at a 1:1 ratio.

Statistics

Comparisons were by t-test with a p-value < 0.05 considered significant. Data were mean ± standard deviation.

Results

Microsphere formation conditions

Reaction of PEG derivatives above the cloud point led to microsphere formation only under specific conditions. To form microspheres at pH 7.4 and 37°C within 45 min, initial reaction of the PEG macromonomers below the cloud point was required ('pre-reaction'). We previously demonstrated that the extent of the crosslinking reaction between eight-arm PEG-vinylsulfone (PEG_8-VS; 10 kDa) and eight-arm PEG-amine (PEG_8-amine; 10 kDa) could be monitored with dynamic light scattering (DLS) [35]. Well before gelation, PEG oligomers/microgels with hydrodynamic radii ≥10 nm were observed by DLS and reached a mean effective diameter (d_{PCS}) of about 180 nm just prior to bulk gelation. To form microspheres, solutions of 10% eight-arm PEG-vinylsulfone (PEG_8-VS; 10 kDa) and 10% PEG-amine (PEG_8-amine; 10 kDa) were pre-reacted for about 6 h at 37°C in PBS ($d_{PCS} \cong 100$ nm), diluted to 2% PEG in PBS + 0.6 M sodium sulfate at room temperature and raised above the cloud point to 37°C. These conditions allowed mixing of polymer and salt at room temperature and did not lead to bulk gelation while the solution was heated to the cloud point. After phase separation, the spherical PEG-rich domains coarsened and crosslinked over the course of 45

min, resulting in the formation of stable PEG microspheres (Suppl. Movie 1). Following buffer exchange into PBS, the microspheres had mean diameters of 6.65±1.65 μm and a polydispersity of 1.59 (Fig. 2a(i)). Other conditions critical for microsphere formation are summarized in Table 1. Pre-reaction was necessary to form microspheres at 37°C within 45 min, but was not necessary if the solutions were heated to 95°C (Suppl. Fig. 1). Vortexing during phase separation led to the formation of a bulk gel consisting of microspheres (Suppl. Fig. 2). Too high of a salt concentration also led to the formation of a bulk gel of microspheres, perhaps due to the large density differences between the phases and rapid 'floating' of the PEG-rich phase (Table 1).

Having found suitable conditions for stable microsphere formation, we then produced degradable PEG microspheres for macropore formation. To fabricate degradable microspheres, eight-arm PEG-acrylate (PEG_8-acrylate; 10 kDa) was reacted with PEG_8-amine. Hydrolysis of the ester bonds present in the microspheres due to the acrylate group provided a mechanism for dissolution of the microspheres [38]. Compared to vinylsulfone, the acrylate group has a slightly lower reactivity toward amines [39]. The slower kinetics of the reaction were overcome by pre-reaction for about 7 h ($d_{PCS} \cong 100$ nm) and incubation for 5 min at 95°C in PBS + 0.45 M sodium sulfate at 2% PEG (Fig. 2a(ii)).

PEG/BSA microspheres were also produced for the delivery of the bioactive lipid S1P. We previously demonstrated that controlled release of S1P from PEG/BSA hydrogels enhances endothelial cell migration [37], and S1P is known to promote angio/vasculogenesis [40,41]. In contrast to the 100% PEG microspheres, production of PEG/BSA microspheres could not be performed at high temperature due to denaturation of the BSA. Formation of microspheres at 37°C required pre-reaction of PEG_8-VS with amine groups on BSA. PEG_8-VS was pre-reacted with BSA for about 6.5 h ($d_{PCS} \cong 100$ nm), followed by incubation for 25 min at 37° C in PBS + 0.65 M sodium sulfate at 0.8% PEG and 1.2% BSA (Fig. 2a(iii)). A negative zeta potential was observed for the PEG/BSA microspheres due to the presence of BSA, while microspheres crosslinked with PEG_8-amine were positively charged (Fig. 2b).

To examine the structure of the microspheres, PEG_8-amine or BSA were fluorescently labeled prior to microsphere formation. Larger microspheres were produced to better visualize the microspheres by using a higher sodium sulfate concentration (0.8 M) to cause phase separation at room temperature. After mixing, solutions were held at room temperature for 5 min before raising the temperature to the values listed above. This protocol produced microspheres with sizes up to about 100 microns in diameter. Microspheres were observed by confocal microscopy, revealing that all three microsphere types were porous (Fig. 2c(i–iii)).

Assembly of modular scaffolds

After formation, microspheres were buffer exchanged into PBS or cell culture medium and reacted to form scaffolds. Unreacted vinylsulfone and amine groups were present on the surfaces of the microspheres, evidenced by the aggregation and crosslinking of microspheres overnight in PBS. To increase the availability of reactive groups for scaffold formation, microspheres were produced with 2:1 or 1:2 ratios of PEG_8-VS to PEG_8-amine. The 2:1 and 1:2 ratio microspheres were mixed in PBS and compacted by centrifugation in UV/vis cuvettes to permit *in situ* visualization by confocal microscopy. Stable scaffolds formed after 200 min at 2000*g*, conditions that may not be favorable for cell survival. However, 2:1 ratio microspheres formed stable scaffolds when centrifuged for 10 min at 1000*g* in the presence of cell culture medium containing 2% serum followed by an overnight incubation at 37°C. The presence of 2% serum was necessary for scaffold formation, indicating that serum proteins served to crosslink the microspheres via reaction of amines on the proteins with vinylsulfone groups on the microspheres. Scaffolds supported their own weight in medium (Fig. 3a) and had storage moduli that were about an order of magnitude lower than bulk hydrogels formed

from the same reactants (Fig. 3b). The storage moduli of the scaffolds were similar to liver tissue and higher than Matrigel or collagen gels [42–45].

The distribution of macropores was controlled by the density (i.e. buoyancy) of the porogenic microspheres relative to the other microsphere types. The density of the PEG_8-acrylate/PEG_8-amine microspheres was changed by varying the length of the reaction at 95°C from 3 min to 10 min during their formation. Upon centrifugation, PEG_8-acrylate/PEG_8-amine microspheres migrated to different locations relative to PEG_8-VS/BSA microspheres, producing gradients in porogenic microspheres (Fig. 4a). If the densities of the different microsphere types were matched by selecting appropriate microsphere formation conditions, scaffolds assembled from PEG_8-VS/PEG_8-amine microspheres and degradable PEG_8-acrylate/PEG_8-amine microspheres demonstrated an even distribution of the two types of microspheres (Fig. 4b). After incubation at 37°C for 2 days, the PEG_8-acrylate microspheres had completely dissolved, leaving behind a porous scaffold of the PEG_8-VS/PEG_8-amine microspheres (Fig. 4c). Some microsphere aggregation prior to scaffold formation was generally observed, but this had the desirable effect of increasing the size and connectivity of macropores that eventually formed in the scaffolds. Assembly of all three types of microspheres with matched densities also led to the formation of scaffolds with evenly distributed pores after two days at 37°C (Fig. 4d).

Cell interactions with scaffolds

The standard scaffold formation conditions were well-tolerated by living cells (1000*g* for 10 min in medium with 2% serum followed by incubation at 37°C overnight). To support cell adhesion, cysteine-containing RGD peptide was conjugated to PEG_8-VS during pre-reaction with PEG_8-amine or BSA [36]. Cell-laden scaffolds were formed by mixing the RGD peptide-derivatized microspheres with degradable microspheres and HepG2 hepatoma cells prior to centrifugation. HepG2 cells were chosen as a surrogate for hepatocytes to assess the feasibility of liver tissue engineering with these scaffolds, as in previous studies [15]. A live/dead assay revealed the viability of HepG2 cells to be minimally impacted by centrifugation in the presence of the microspheres (93.64 ± 3.34% live cells). Dissolution of porogenic microspheres over the course of two days in culture had no further effect on the survival of the HepG2 cells (91.94 ± 1.87% live cells), demonstrating that the degradation products of the porogenic microspheres were not cytotoxic (Fig. 5a). The cells were evenly distributed in the scaffolds and surrounded by but not encapsulated within microspheres (Fig. 5b). Viability after three weeks in culture was lower, 43.4± 9. 7% live cells, with medium changes every two days.

The potential for directed vascularization into the modular scaffolds was assessed by observing the infiltration of human aortic endothelial cells after dissolution of the porogen. Due to the formation of a tight seal between the scaffolds and the sides of UV/vis cuvettes, endothelial cell migration only occurred from the top of the scaffold (Suppl. Figs. 3 & 4). For confocal microscopy, the cuvettes were turned on their sides to allow imaging along the entire length of the scaffold to a maximum observable depth of about 300 microns. The influence of macroporosity on endothelial cell infiltration was investigated by introducing gradients of porosity into scaffolds, which resulted in a highly porous 250–300 μm upper layer and a less porous lower layer (Fig. 6a). With RGD peptide incorporated in the scaffold, endothelial cells (red) penetrated throughout the highly porous upper layer within 24 h (Fig. 6a(i)) and continued to migrate into the less porous lower region by 48 h (Fig. 6a(ii)). No endothelial cell infiltration was found when the scaffolds were formed without the porogenic microspheres (Fig. 6a(iii)). With high porosity but no RGD peptide, endothelial cells were found only at the top of the scaffold, illustrating that settling alone is not sufficient for infilration (Fig. 6a(iv)). To specifically probe the influence of S1P release, endothelial cell migration rates into scaffolds with uniform porosity were compared with and without loading of S1P into the PEG_8-VS/BSA

microspheres (Fig. 6b). The rate of endothelial cell migration increased from 2.6 ± 0.8 μm/h to 5.4 ± 1.0 μm/h when S1P was delivered from PEG/BSA microspheres ($p < 1x10^{-5}$).

Finally, we observed the infiltration of endothelial cells into scaffolds containing HepG2 cells. The scaffolds formed with HepG2 cells and all three microsphere types were cultured for two days to allow pore formation by dissolution of the PEG_8-acrylate/PEG_8-amine microspheres. Scaffolds were dislodged from the cuvettes to permit endothelial cell infiltration from all sides of the scaffolds. The HepG2 cells within these scaffolds were labeled with Vybrant DiO (green) while the endothelial cells were labeled with Vybrant DiI (red). The PEG_8-VS/BSA microspheres were labeled with Dylight 633 (blue). With conjugated RGD peptide, endothelial cell migration was observed after two days up to the maximum imaging depth of 300 μm, with and without delivery of S1P (Fig. 7).

Discussion

In this study, we introduce a new method of constructing tissue engineering scaffolds from PEG-based microspheres. The method is highly scalable and amenable to macroporous scaffold formation in the presence of living cells. Khademhossein et al. recently categorized different methods of forming hydrogel scaffolds as either “top-down”, i.e. pore formation followed by cell seeding, or “bottom-up”, i.e. assembly of cell-laden hydrogel modules [13, 19]. The present strategy does not fit either description but combines beneficial aspects of both top-down and bottom-up strategies. Similar to top-down strategies, macropores for cell infiltration are produced using a degradable porogen. Unlike the commonly used porogens, PEG_8-acrylate/PEG_8-amine microspheres are non-cytotoxic and form macropores in the presence of cells. Similar to bottom-up strategies, the scaffolds are assembled from smaller modules. However, the modules may be assembled around cells due to their small size and do not require encapsulation of cells within crosslinked bulk hydrogel. Assembly of microspheres around cells may enhance transport of nutrients and facilitate removal of waste products. *In situ* macropore formation may further enhance transport, even more so if directed vascularization of scaffolds could be promoted. Additionally, the ability to produce microsphere gradients may be useful to introduce gradients in mechanical stiffness or bioactive factors to influence cellular responses to the scaffolds. Gradients in these properties may have applications in both the transplantation of cells *in vivo* and the differentiation of stem cells *in vitro* [46–48]. However, an increase in the stiffness/toughness of the current scaffolds would aid in the handling of the scaffolds and allow engineering of tissue such as bone or cartilage. Furthermore, the use of serum proteins to crosslink the microspheres may enhance the immune response *in vivo*. Alternative strategies to crosslink the microspheres may address both concerns.

The method of microsphere formation is similar to the coacervation method commonly used to form gelatin microcapsules for drug encapsulation [49]. Gelatin is usually phase separated from water using ethanol (solvent-induced) or sodium sulfate (thermally induced). Although the term coacervation is not typically used with polymers, the processes are thermodynamically indistinguishable. In the standard protocol for the production of gelatin microspheres, size is controlled by rapidly stirring the solution in the presence of a stabilizer. Upon cooling, the gelatin solidifies. The gelatin microspheres are then crosslinked with formaldehyde or other agents to prevent rapid re-dissolution of the microspheres in water. An important distinction between the current method and the gelatin method are that the PEG microspheres cannot be solidified by cooling and must be crosslinked *in situ*. However, due to the ability to manipulate the crosslinking kinetics, micron-sized PEG microspheres may be produced in the absence of mixing or stabilizers. The technique, with modifications, should be applicable to other crosslinkable polymers that exhibit a thermally induced phase separation.

The current technique has some similarities to previous methods. Gelatin microspheres formed by an emulsion process were previously used as porogens by the Mikos group [50]. Recently, PEG-sebacic acid-diacrylate was used to form hydrogel microspheres by an emulsion process. These were used as slowly dissolving porogens, but not in the presence of living cells [51]. Irvine and colleagues used saturated sodium chloride solutions to form aqueous emulsions of PEG-methacrylate with the PEG-based surfactant Pluronic F-68 [52]. Martin & Vermette reacted mono-activated PEG stirred above the cloud point in sodium sulfate with amine-containing surfaces to produce low protein-fouling surfaces [53]. In addition to salts, phase separation of PEG may also be effected by the presence of dextran and used to produce microspheres or scaffolds in an all-aqueous system. Hennink and colleagues demonstrated that vigorously mixed, phase separated all-aqueous solutions of PEG and dextran could be polymerized by free-radical polymerization, resulting in crosslinked dextran or PEG microspheres [34,54]. Dextran microspheres were produced with charged or hydrophobic groups, which allowed non-covalent assembly of microspheres into scaffolds upon mixing of lyophilized microspheres prior to addition of buffered water [55–57]. The sizes and polydispersities of the microspheres were found to affect the stiffness of the formed scaffolds [58]. Their results suggest that polydispersity in microsphere sizes may be beneficial, but only if the smaller microspheres efficiently pack in the gaps between larger microspheres. Another PEG/dextran strategy has been used to directly form macroporous dextran scaffolds, as demonstrated by Shoichet and colleagues [10]. It was proposed that the scaffolds consisted of dextran microspheres gelled together, similar to the bulk gel of microspheres observed under some conditions here. Comparing the current method to the dextran/PEG method, sodium sulfate is less expensive and perhaps more easily removed than dextran. Additionally, formation of microspheres in the absence of mixing may be more challenging with free-radical polymerization, because although polymerization occurs rapidly, initiation will often be a heterogeneous process and may occur over a relatively long period of time.

Conclusions

The methods presented here for fabricating PEG microspheres advances the modular approach to the design of tissue engineering scaffolds. By assembling multiple types of hydrogel microspheres with diverse properties, we developed a highly scalable platform designed to enhance biocompatibility while allowing control over bioactivity and porosity. Scalability resulted from solution-phase synthesis of microspheres, while biocompatibility was enhanced by the absence of surfactants, organic solvents and other additives. The enhanced biocompatibility allowed assembly of scaffolds in the presence of cells, resulting in a homogenous cellular distribution. Bioactivity was introduced via RGD peptide conjugation and S1P delivery, both of which promoted endothelial cell infiltration. The use of porogenic microspheres with different densities allowed introduction of gradients in macroporosity, suggesting the potential to develop highly complex scaffolds. Production of libraries of PEG microsphere with distinct properties may allow the development of advanced scaffolds with application-specific architectures, bioactivity, mechanical properties and degradation kinetics.

Supplementary Material

Refer to Web version on PubMed Central for supplementary material.

Acknowledgments

The authors are grateful to Igor Efimov for use of the confocal microscope and funding from NIH R01HL085364 (DLE) and American Heart Association Predoctoral Fellowship 0715676Z (EAS).

References

1. Tessmar JK, Göpferich AM. Customized PEG-Derived Copolymers for Tissue-Engineering Applications. Macromolecular Bioscience 2007;7:23–39. [PubMed: 17195277]
2. Drury JL, Mooney DJ. Hydrogels for tissue engineering: Scaffold design variables and applications. Biomaterials 2003;24:4337–51. [PubMed: 12922147]
3. Lutolf MP, Hubbell JA. Synthetic biomaterials as instructive extracellular microenvironments for morphogenesis in tissue engineering. Nat Biotech 2005;23:47–55.
4. Varghese S, Elisseeff JH. Hydrogels for musculoskeletal tissue engineering. Polymers for Regenerative Medicine 2006:95–144.
5. Hill E, Boontheekul T, Mooney DJ. Designing Scaffolds to Enhance Transplanted Myoblast Survival and Migration. Tissue Engineering 2006;12:1295–304. [PubMed: 16771642]
6. Shapiro L, Cohen S. Novel alginate sponges for cell culture and transplantation. Biomaterials 1997;18:583–90. [PubMed: 9134157]
7. Stachowiak AN, Bershteyn A, Tzatzalos E, Irvine DJ. Bioactive Hydrogels with an Ordered Cellular Structure Combine Interconnected Macroporosity and Robust Mechanical Properties. Advanced Materials 2005;17:399–403.
8. Bryant SJ, Cuy JL, Hauch KD, Ratner BD. Photo-patterning of porous hydrogels for tissue engineering. Biomaterials 2007;28:2978–86. [PubMed: 17397918]
9. Sannino A, Netti PA, Madaghiele M, Coccoli V, Luciani A, Maffezzoli A, et al. Synthesis and characterization of macroporous poly(ethylene glycol)-based hydrogels for tissue engineering application. Journal of Biomedical Materials Research Part A 2006;79A:229–36. [PubMed: 16752396]
10. Lévesque SG, Lim RM, Shoichet MS. Macroporous interconnected dextran scaffolds of controlled porosity for tissue-engineering applications. Biomaterials 2005;26:7436–46. [PubMed: 16023718]
11. Ford MC, Bertram JP, Hynes SR, Michaud M, Li Q, Young M, et al. A macroporous hydrogel for the coculture of neural progenitor and endothelial cells to form functional vascular networks in vivo. Proceedings of the National Academy of Sciences of the United States of America 2006;103:2512–7. [PubMed: 16473951]
12. Osathanon T, Linnes ML, Rajachar RM, Ratner BD, Somerman MJ, Giachelli CM. Microporous nanofibrous fibrin-based scaffolds for bone tissue engineering. Biomaterials 2008;29:4091–9. [PubMed: 18640716]
13. Rivest C, Morrison DWG, Ni B, Rubin J, Yadav V, Mahdavi A, et al. Microscale hydrogels for medicine and biology: Synthesis, characteristics and applications. Journal of Mechanics of Materials and Structures 2007;2:1103–19.
14. Serban MA, Prestwich GD. Modular extracellular matrices: solutions for the puzzle. Methods (San Diego, Calif 2008;45:93–8.
15. McGuigan AP, Sefton MV. Vascularized organoid engineered by modular assembly enables blood perfusion. Proceedings of the National Academy of Sciences 2006;103:11461–6.
16. Yeh J, Ling Y, Karp JM, Gantz J, Chandawarkar A, Eng G, et al. Micromolding of shape-controlled, harvestable cell-laden hydrogels. Biomaterials 2006;27:5391–8. [PubMed: 16828863]
17. Du Y, Lo E, Ali S, Khademhosseini A. Directed assembly of cell-laden microgels for fabrication of 3D tissue constructs. Proceedings of the National Academy of Sciences 2008;105:9522–7.
18. Pautot S, Wyart C, Isacoff EY. Colloid-guided assembly of oriented 3D neuronal networks. Nat Meth 2008;5:735–40.
19. Khademhosseini A, Langer R. Microengineered hydrogels for tissue engineering. Biomaterials 2007;28:5087–92. [PubMed: 17707502]
20. Boland T, Xu T, Damon B, Cui X. Application of inkjet printing to tissue engineering. Biotechnology Journal 2006;1:910–7. [PubMed: 16941443]
21. Lu Y, Mapili G, Suhali G, Chen S, Roy K. A digital micro-mirror device-based system for the microfabrication of complex, spatially patterned tissue engineering scaffolds. Journal of biomedical materials research 2006;77:396–405. [PubMed: 16444679]
22. Tsang VL, Bhatia SN. Three-dimensional tissue fabrication. Advanced Drug Delivery Reviews 2004;56:1635–47. [PubMed: 15350293]

23. Um E, Lee D-S, Pyo H-B, Park J-K. Continuous generation of hydrogel beads and encapsulation of biological materials using a microfluidic droplet-merging channel. Microfluidics and Nanofluidics 2008;5:541–9.
24. Tan WH, Takeuchi S. Monodisperse alginate hydrogel microbeads for cell encapsulation. Advanced Materials 2007:2696–+.19
25. Kim JW, Utada AS, Fernandez-Nieves A, Hu ZB, Weitz DA. Fabrication of monodisperse gel shells and functional microgels in microfluidic devices. Angew Chem-Int Edit 2007;46:1819–22.
26. Leobandung W, Ichikawa H, Fukumori Y, Peppas NA. Preparation of stable insulin-loaded nanospheres of poly(ethylene glycol) macromers and N-isopropyl acrylamide. J Control Release 2002;80:357–63. [PubMed: 11943411]
27. Nolan CM, Reyes CD, Debord JD, Garcia AJ, Lyon LA. Phase transition behavior, protein adsorption, and cell adhesion resistance of poly(ethylene glycol) cross-linked microgel particles. Biomacromolecules 2005;6:2032–9. [PubMed: 16004442]
28. Kawaguchi H, Fujimoto K, Mizuhara Y. Hydrogel microspheres III. Temperature-dependent adsorption of proteins on poly-N-isopropylacrylamide hydrogel microspheres. Colloid & Polymer Science 1992;270:53–7.
29. Jeon S, Lee J, Andrade J, DeGennes P. Protein Surface Interactions in the Presence of Polyethylene Oxide.1. Simplified Theory. Journal of Colloid and Interface Science 1991;142:149–58.
30. Prime KL, Whitesides GM. Self-assembled organic monolayers: model systems for studying adsorption of proteins at surfaces. Science 1991;252:1164–7.
31. Bailey FE, Callard RW. Some properties of poly(ethylene oxide) in aqueous solution. J Appl Polym Sci 1959;1:56–62.
32. Bae YC, Lambert SM, Soane DS, Prausnitz JM. Cloud-Point Curves of Polymer-Solutions from Thermooptic Measurements. Macromolecules 1991;24:4403–7.
33. Yen DR, Raghavan S, Merrill EW. Fractional precipitation of star poly(ethylene oxide). Macromolecules 1996;29:8977–8.
34. Franssen O, Hennink WE. A novel preparation method for polymeric microparticles without the use of organic solvents. International Journal of Pharmaceutics 1998;168:1–7.
35. Scott EA, Nichols MD, Cordova LH, George BJ, Jun Y-S, Elbert DL. Protein adsorption and cell adhesion on nanoscale bioactive coatings formed from poly(ethylene glycol) and albumin microgels. Biomaterials 2008;29:4481–93. [PubMed: 18771802]
36. Elbert DL, Hubbell JA. Conjugate Addition Reactions Combined with Free-radical Cross-linking for the Design of Materials for Tissue Engineering. Biomacromolecules 2001;2:430–41. [PubMed: 11749203]
37. Wacker BK, Scott EA, Kaneda MM, Alford SK, Elbert DL. Delivery of sphingosine 1-phosphate from poly(ethylene glycol) hydrogels. Biomacromolecules 2006;7:1335–43. [PubMed: 16602758]
38. Elbert DL, Pratt AB, Lutolf MP, Halstenberg S, Hubbell JA. Protein delivery from materials formed by self-selective conjugate addition reactions. J Control Release 2001;76:11–25. [PubMed: 11532309]
39. Friedman M, Cavins JF, Wall JS. Relative Nucleophilic Reactivities of Amino Groups and Mercaptride Ions in Addition Reactions with alpha, beta-Unsaturated Compounds. Journal of American Chemical Society 1965;87:3672–82.
40. Ancellin N, Colmont C, Su J, Li Q, Mittereder N, Chae SS, et al. Extracellular export of sphingosine kinase-1 enzyme. Sphingosine 1-phosphate generation and the induction of angiogenic vascular maturation. J Biol Chem 2002;277:6667–75. [PubMed: 11741921]
41. Sefcik LS, Petrie Aronin CE, Wieghaus KA, Botchwey EA. Sustained release of sphingosine 1-phosphate for therapeutic arteriogenesis and bone tissue engineering. Biomaterials 2008;29:2869–77. [PubMed: 18405965]
42. Levental I, Georges PC, Janmey PA. Soft biological materials and their impact on cell function. Soft Matter 2007;3:299–306.
43. Raeber GP, Lutolf MP, Hubbell JA. Molecularly Engineered PEG Hydrogels: A Novel Model System for Proteolytically Mediated Cell Migration. 2005;89:1374–88.

44. Cullen D, Lessing M, LaPlaca M. Collagen-Dependent Neurite Outgrowth and Response to Dynamic Deformation in Three-Dimensional Neuronal Cultures. Annals of Biomedical Engineering 2007;35:835–46. [PubMed: 17385044]
45. Lai G, Li Y, Li G. Effect of concentration and temperature on the rheological behavior of collagen solution. International Journal of Biological Macromolecules 2008;42:285–91. [PubMed: 18275999]
46. Engler AJ, Griffin MA, Sen S, Bonnemann CG, Sweeney HL, Discher DE. Myotubes differentiate optimally on substrates with tissue-like stiffness: pathological implications for soft or stiff microenvironments. J Cell Biol 2004;166:877–87. [PubMed: 15364962]
47. Moore K, Macsween M, Shoichet M. Immobilized Concentration Gradients of Neurotrophic Factors Guide Neurite Outgrowth of Primary Neurons in Macroporous Scaffolds. Tissue Engineering 2006;12:267–78. [PubMed: 16548685]
48. DeLong SA, Moon JJ, West JL. Covalently immobilized gradients of bFGF on hydrogel scaffolds for directed cell migration. Biomaterials 2005;26:3227–34. [PubMed: 15603817]
49. Arshady R. Microspheres and microcapsules, a survey of manufacturing techniques. 2. coacervation. Polym Eng Sci 1990;30:905–14.
50. Holland TA, Tessmar JK, Tabata Y, Mikos AG. Transforming growth factor-beta 1 release from oligo (poly(ethylene glycol) fumarate) hydrogels in conditions that model the cartilage wound healing environment. J Control Release 2004;94:101–14. [PubMed: 14684275]
51. Kim J, Yaszemski MJ, Lu L. Three-Dimensional Porous Biodegradable Polymeric Scaffolds Fabricated with Biodegradable Hydrogel Porogens. Tissue Engineering Part C: Methods. 10.1089/ten.tec.2008.0642
52. Jain S, Yap WT, Irvine DJ. Synthesis of Protein-Loaded Hydrogel Particles in an Aqueous Two-Phase System for Coincident Antigen and CpG Oligonucleotide Delivery to Antigen-Presenting Cells. Biomacromolecules 2005;6:2590–600. [PubMed: 16153096]
53. Martin Y, Vermette P. Low-fouling amine-terminated poly(ethylene glycol) thin layers and effect of immobilization conditions on their mechanical and physicochemical properties. Macromolecules 2006;39:8083–91.
54. Van Thienen TG, Demeester J, De Smedt SC. Screening poly(ethyleneglycol) micro-and nanogels for drug delivery purposes. International Journal of Pharmaceutics 2008;351:174–85. [PubMed: 18061378]
55. Van Tomme SR, van Steenbergen MJ, De Smedt SC, van Nostrum CF, Hennink WE. Self-gelling hydrogels based on oppositely charged dextran microspheres. Biomaterials 2005;26:2129–35. [PubMed: 15576188]
56. Van Tomme SR, Mens A, van Nostrum CF, Hennink WE. Macroscopic Hydrogels by Self-Assembly of Oligolactate-Grafted Dextran Microspheres. Biomacromolecules 2008;9:158–65. [PubMed: 18081253]
57. Van Tomme SR, Storm G, Hennink WE. In situ gelling hydrogels for pharmaceutical and biomedical applications. International Journal of Pharmaceutics 2008;355:1–18. [PubMed: 18343058]
58. Van Tomme SR, van Nostrum CF, Dijkstra M, De Smedt SC, Hennink WE. Effect of particle size and charge on the network properties of microsphere-based hydrogels. European Journal of Pharmaceutics and Biopharmaceutics 2008;70:522–30. [PubMed: 18582574]

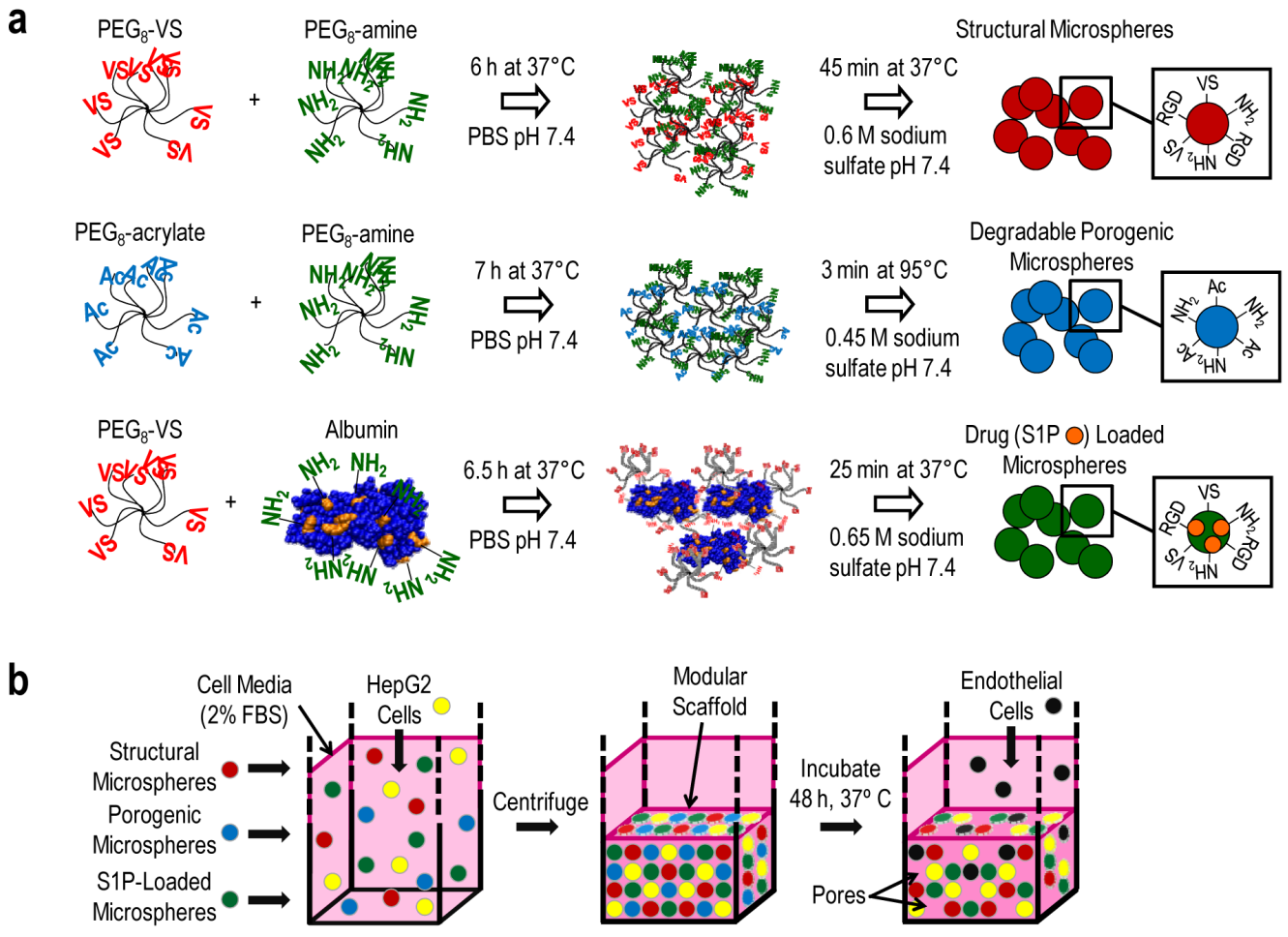

Figure 1.

Production of microspheres and their assembly into bioactive modular scaffolds. (**a**) Eight-arm PEG-vinylsulfone (PEG_8-VS) was reacted with eight-arm PEG-amine (PEG_8-amine) in PBS. The Michael-type reaction was followed by dynamic light scattering to detect the formation of PEG oligomers/microgels during crosslinking. At a certain mean effective diameter (d_{PCS}), sodium sulfate was added and the solution was heated above the cloud point. A similar strategy was followed with eight arm PEG-acrylate (PEG_8-acrylate) and PEG_8-amine to produce porogenic microspheres. Microspheres were produced for the delivery of sphingosine 1-phosphate (S1P) to promote endothelial cell migration by reacting PEG_8-VS with bovine serum albumin (BSA). (**b**), Microspheres with different functionalities were mixed with HepG2 hepatoma cells in medium containing 2% serum and centrifuged for 10 min at 1000*g* and allowed to crosslink overnight at 37°C. Within 48 h, PEG_8-acrylate/PEG_8-amine microspheres dissolved to form macroporous scaffolds. Endothelial cells seeded on the scaffolds adhered via RGD peptide incorporated in the non-degradable microspheres.

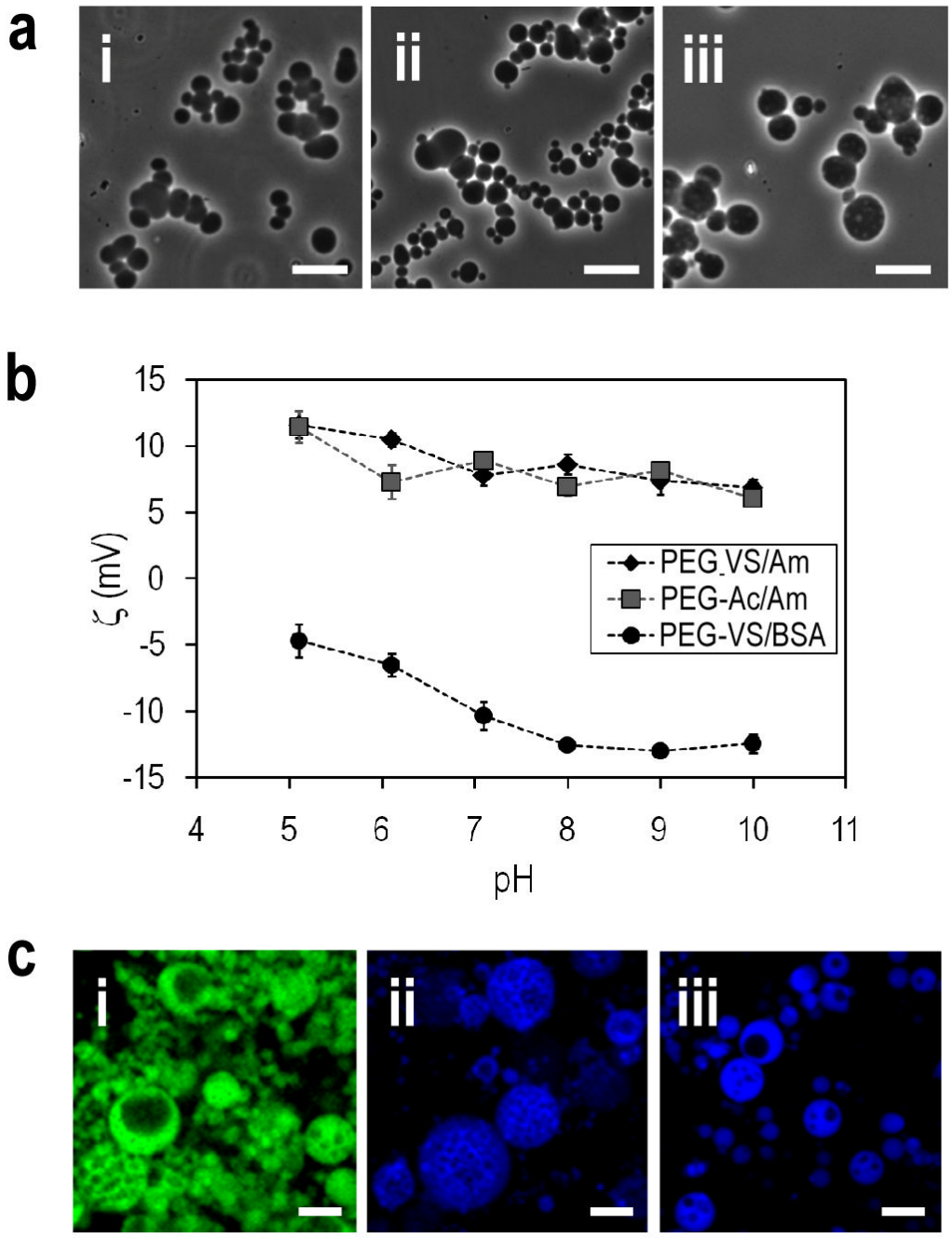

Figure 2.

PEG or PEG/BSA microspheres were formed above the cloud point and then buffer exchanged into PBS. (**a**) Phase-contrast photomicrographs with a 20X objective of: (**i**) PEG_8-VS/PEG_8-amine (**ii**) PEG_8-acrylate/PEG_8-amine and (**iii**) PEG_8-VS/BSA microspheres. Scale bar = 10μm. (**b**) Zeta potentials of the three types of microspheres. The net charge was positive if PEG_8-amine was used to crosslink the microspheres, while the net charge was negative if BSA was used as the crosslinker. (c) Confocal microscopy with a 10X objective of: (**i**) PEG_8-VS/PEG_8-amine (**ii**) PEG_8-acrylate/PEG_8-amine and (**iii**) PEG_8-VS/BSA microspheres. Microspheres were formed under conditions that produced larger microspheres to aid in visualizing their porous structure. Scale bar = 50μm.

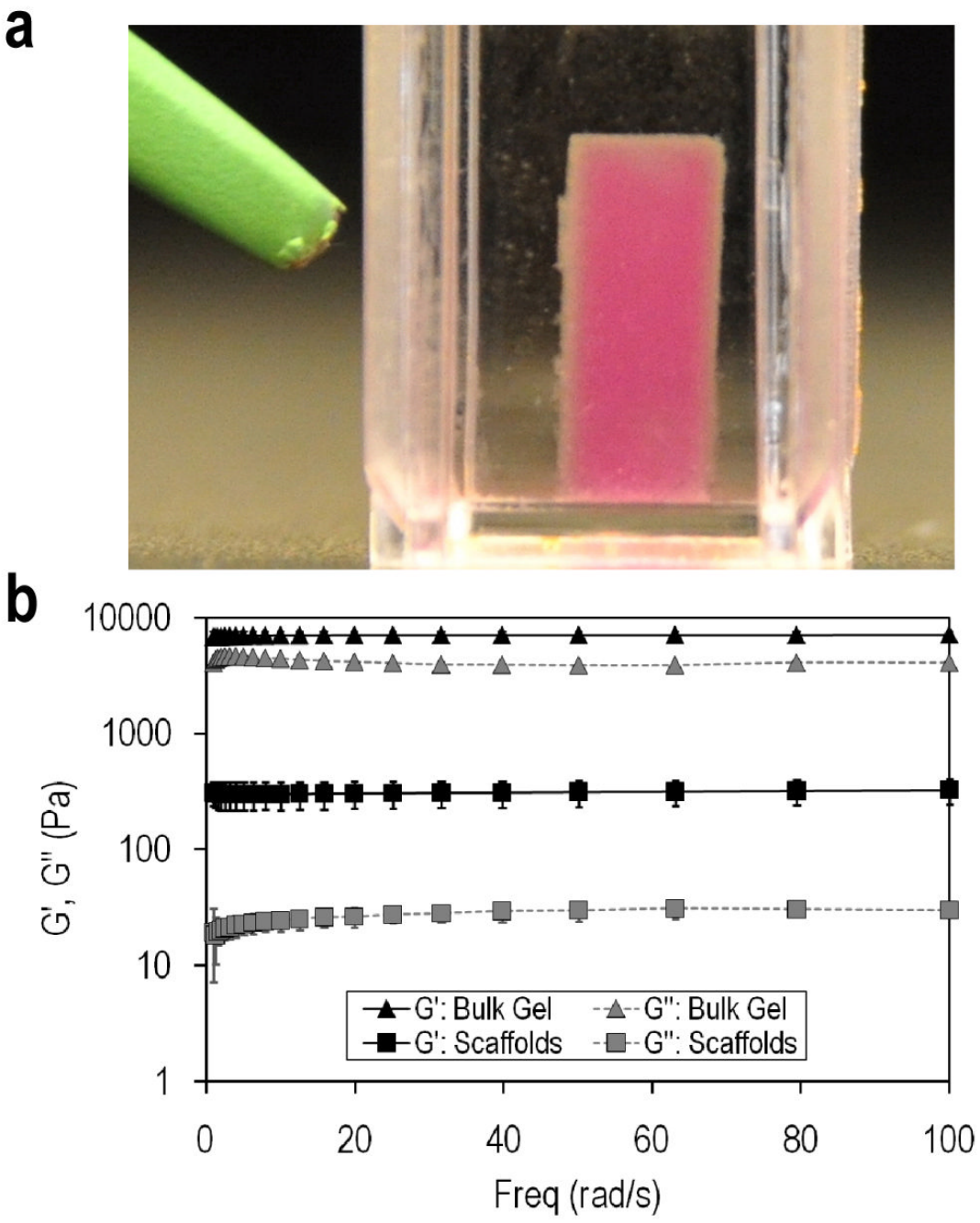

Figure 3.

Scaffolds may be formed by centrifuging microspheres in the presence of 2% serum. (**a**) Photograph of a scaffold composed of PEG_8-VS/PEG_8-amine microspheres, PEG_8-acrylate/PEG_8-amine microspheres and PEG_8-VS/BSA microspheres. Microspheres were compacted by centrifugation at 1000*g* for 10 min in the presence of HepG2 hepatoma cells and then incubated for 12 h at 37°C in medium with 2% FBS. (**b**) Rheometric measurements of storage (G') and loss (G") moduli of modular scaffolds formed from PEG_8-VS/PEG_8-amine microspheres compared with bulk hydrogels formed by crosslinking PEG_8-VS with PEG_8-amine below the cloud point.

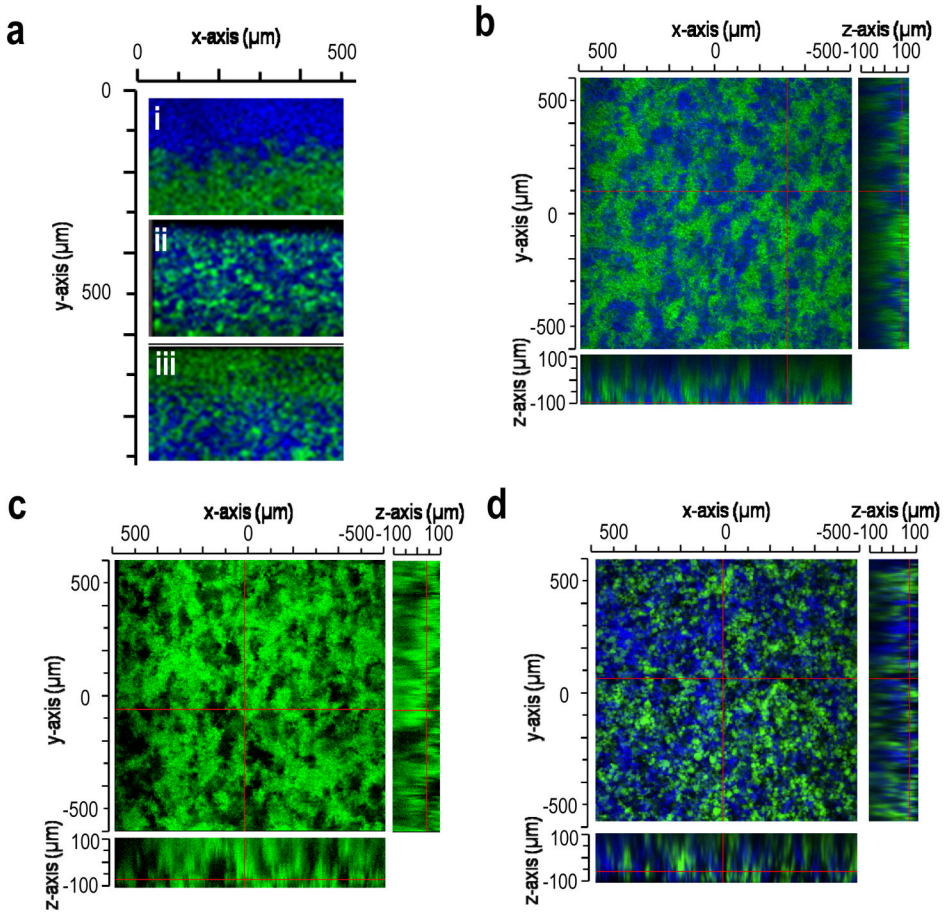

Figure 4.

Macroporosity was introduced in the presence of cells via dissolution of porogenic microspheres. Images were obtained by confocal microscopy with a 10X objective. (**a**) Scaffolds could be formed with gradients of microspheres by centrifuging PEG_8-VS/BSA microspheres (green) with (**i**) low, (**ii**) medium or (**iii**) high density PEG_8-acrylate/PEG_8-amine microspheres (blue). The density of the PEG_8-acrylate/PEG_8-amine microspheres was varied by reacting solutions of PEG_8-acrylate and PEG_8-amine in PBS + 0.45 M sodium sulfate at 95°C for: (**i**) 3 min, (**ii**) 5 min or (**iii**) 10 min. (**b**) A scaffold formed from PEG_8-VS/PEG_8-amine microspheres (green) and PEG_8-acrylate/PEG_8-amine microspheres (blue) with matched densities, imaged 12 h after centrifugation in cell culture medium at 37°C. (**c**) Scaffold from (b) after 48 h in cell culture medium at 37°C. PEG_8-acrylate/PEG_8-amine microspheres (blue) were no longer detectable. (**d**) Macroporous scaffold composed of PEG_8-VS/PEG_8-amine microspheres (green), PEG_8-acrylate/PEG_8-amine microspheres PEG_8-VS/BSA microspheres (blue), 48 h after formation. Microsphere densities were matched to produce an even distribution of macropores following dissolution of PEG_8-acrylate/PEG_8-amine microspheres.

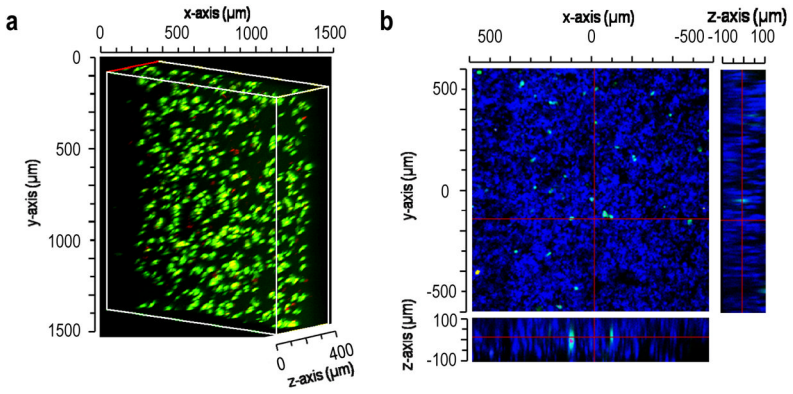

Figure 5.

Scaffolds could be formed in the presence of cells. (**a**) HepG2 cell viability in a scaffold composed of PEG_8-VS/PEG_8-amine microspheres, PEG_8-acrylate/PEG_8-amine microspheres (blue) and PEG_8-VS/BSA microspheres. The PEG_8-acrylate/PEG_8-amine microspheres were no longer detectable, demonstrating complete hydrolysis of porogenic microspheres. HepG2 cells were stained with fluorescein diacetate (green; live) and ethidium bromide (red; dead). (**b**) HepG2 cell viability in a scaffold similar to (a) but composed of PEG_8-VS/PEG_8-amine microspheres, PEG_8-VS/BSA microspheres (blue) and PEG_8-acrylate/PEG_8-amine microspheres. HepG2 cells were evenly dispersed throughout the macroporous scaffold and were surrounded by microspheres but not encapsulated in them. Live/dead assays were performed 48 h after scaffold formation to allow porogen dissolution, revealing cell viability of 91.9 ± 1.87% (*n*=3). Cells were imaged by confocal microscopy with a 10X objective.

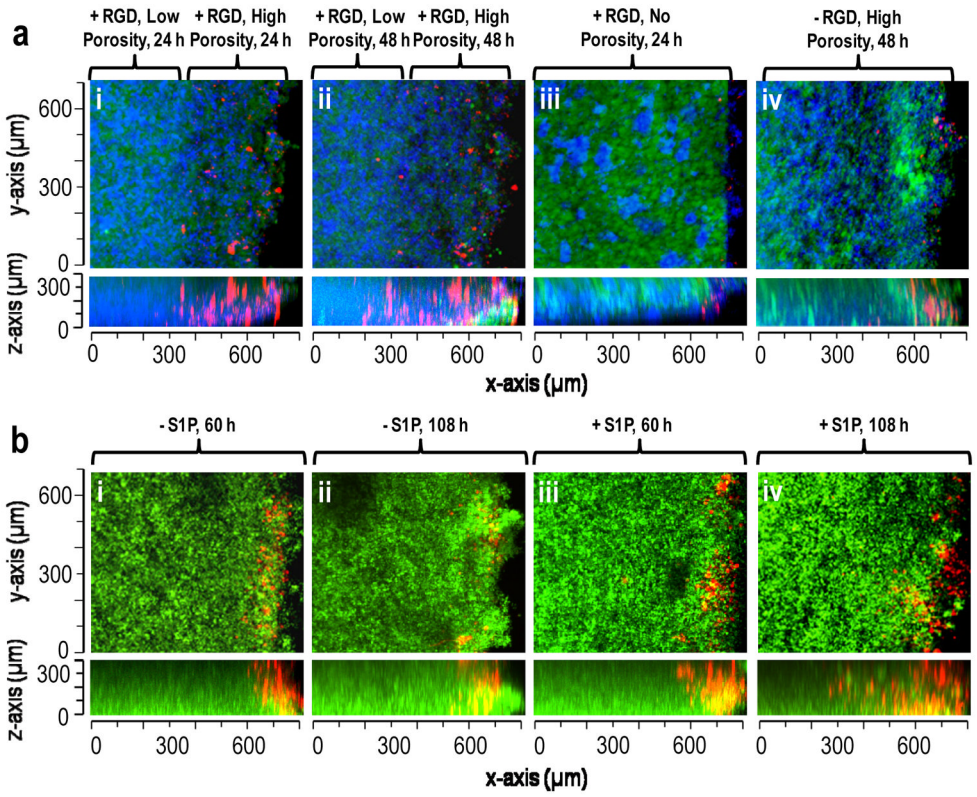

Figure 6.

S1P, porosity and RGD peptide affected endothelial cell migration in modular scaffolds. (**a**) Migration of Vybrant DiI stained endothelial cells (red) into scaffolds composed of PEG_8-VS/PEG_8-amine microspheres (green), PEG_8-acrylate/PEG_8-amine microspheres and PEG_8-VS/BSA microspheres (blue). Scaffolds were formed with: (**i**) RGD peptide and a highly porous 250–300 μm upper layer, imaged 24 h after cell seeding, (**ii**) Same location within scaffold from (i) at 48 h, (**iii**) RGD peptide but no porogenic microspheres, 24 h, (**iv**) No RGD peptide but with porogenic microspheres, 48 h. (**b**) Migration of endothelial cells (red) into scaffolds with uniform porosity composed of PEG_8-VS/PEG_8-amine microspheres, PEG_8-acrylate/PEG_8-amine microspheres and PEG_8-VS/BSA microspheres (with or without S1P-loaded, green): (**i**) 60 h after cell seeding without S1P-loading, (**ii**) 108 h without S1P-loading, (**iii**) 60 h with S1P-loading, (**iv**) 108 h with S1P-loading. The maximum extent of migration of endothelial cells was recorded at 50 μm increments within each scaffold. The average rate of migration increased from 2.57±0.76 μm/h to 5.4±1.02 μm/h when S1P was released from the PEG_8-VS/BSA microspheres.

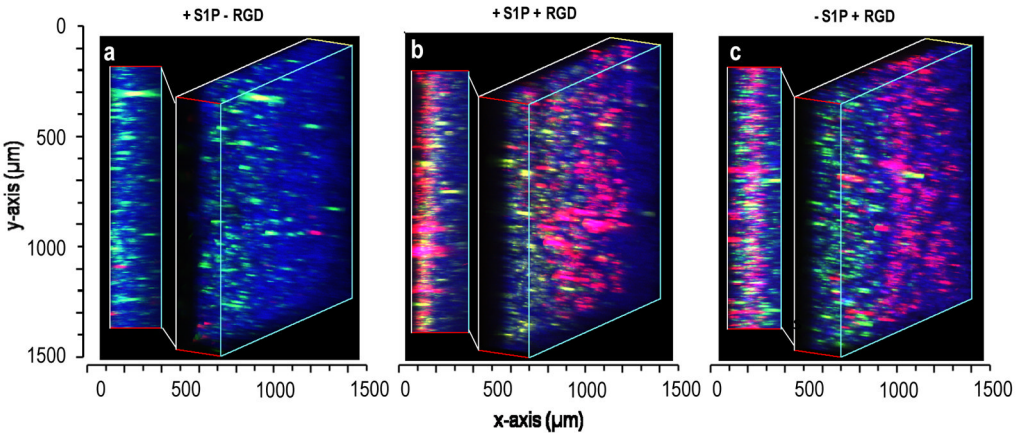

Figure 7.

Endothelial migration into scaffolds containing HepG2 cells. Modular scaffolds were formed from all three types of microspheres in the presence of HepG2 cells stained with Vybrant DiO (green). After crosslinking with media proteins and hydrolysis of porogenic microspheres for 48 h, endothelial cells (red) were seeded onto all sides of the scaffolds. The scaffolds contained: (**i**) S1P-loaded PEG_8-VS/BSA microspheres (blue) without RGD peptide, (**ii**) PEG_8-VS/BSA microspheres (blue) loaded with S1P, with RGD, (**iii**) PEG_8-VS/BSA microspheres (blue) not loaded with S1P, with RGD. Cells were imaged by confocal microscopy with a 10X objective. Endothelial cells migrated to the maximum observable distance (300 μm) within two days with or without S1P delivery. Scaffolds were imaged by confocal microscopy with a 10X objective.

Table 1

Summary of products resulting from microsphere fabrication methods

Salt conc. (M sodium sulfate +PBS; pH 7.4)	Pre-reaction (below the cloud point) (d_{PCS})	Reaction temperature and time (above the cloud point)	Result	Image
		PEG_8-vinylsulfone/PEG_8-amine		
0.6	None	37°C, 45 min	No microspheres or gel	-
0.6	None	37°C, overnight	Bulk gel of microspheres	Suppl. Fig. 1a
0.6	None	95°C, 3 min	Microspheres	Suppl. Fig. 1b
0.6	100 nm	95°C, 3 min	Microspheres	Suppl. Fig. 1c
0.6	100 nm	37°C, 45 min	Microspheres	Fig. 2a(i)
0.6	100 nm	37°C, 45 min, with 5 min vortex	Bulk gel with irregular structure	Suppl. Fig. 2
1.5	None	95°C, 5 min	Bulk gel of microspheres	-
1.5	100 nm	95°C, 5 min	Bulk gel of microspheres	-
		PEG_8-acrylate/PEG_8-amine		
0.45	100 nm	95°C, 10 min	High density microspheres*	Fig. 4a
0.45	100 nm	95°C, 5 min	Medium density microspheres*	Fig. 2a(ii), 4a
0.45	100 nm	95°C, 3 min	Low density microspheres*	Fig. 4a
		PEG_8-vinylsulfone/BSA		
0.65	100 nm	37°C, 25 min	Medium density microspheres*	Fig.2a(iii)
0.65	100 nm	95°C, 10 min	Denatured BSA	-

*Density is relative to PEG8-vinylsulfone/PEG8-amine microspheres (d_{PCS} = 100 nm, 45 min at 37°C in PBS + 0.6 M sodium sulfate)